

## Application Report

# High throughput screening for mode-of-action on Na<sub>v</sub>1.4

Qube, an ideal tool for profiling large compound libraries on voltage-gated sodium channels.

### Summary

- Constantly high success rates (99% in three experiments)
- Giga-ohm seal resistances in almost all wells
- Very low data spread
  - All CV values of DMSO control below 10%
  - No false positives with cut-off criteria 3 X SD
  - Z' constantly greater 0.75
- Discrimination between different modes of inhibition (state-dependency)
- Up to 384 individual IC<sub>50</sub> values (3072 data points) determined in just one experiment
- Using Qube in combination with stacker it would be possible to determine up to 7680 IC<sub>50</sub> (60,000 data points) per 24 hours.



### Introduction

Voltage-gated sodium channels (VGSC) play a pivotal role in initiating and propagating action potentials in excitable cells. The family of VGSC consists of 9 known, human  $\alpha$ -subunits (Na<sub>v</sub>1.1 – 9) that exhibit a high degree of sequence homology. Similar biophysical and pharmacological properties among the different subtypes are a result of this homology (Yu & Catterall, 2003). VGSC have long been in the focus of drug development as their activity was linked to neuronal disorders including epilepsy and chronic pain. The relevance of these channels was further boosted by recent studies that have revealed further roles of VGSC in health and disease such as autism, migraine, multiple sclerosis, cancer as well as muscle and immune system dysfunctions (Eijkelkamp et al., 2012).

Na<sub>v</sub>1.4 is encoded by the SCN4A gene and is predominantly expressed in skeletal muscles. The channel is driving depolarization of the membrane potential in these cells and is thereby responsible for propagation of the action potential that eventually controls muscle contraction. There are currently 5 mutations in the SCN4A gene described that are either linked to hypertonia (myotonia) or to muscle weakness (Jurkat-Rott et al., 2010).

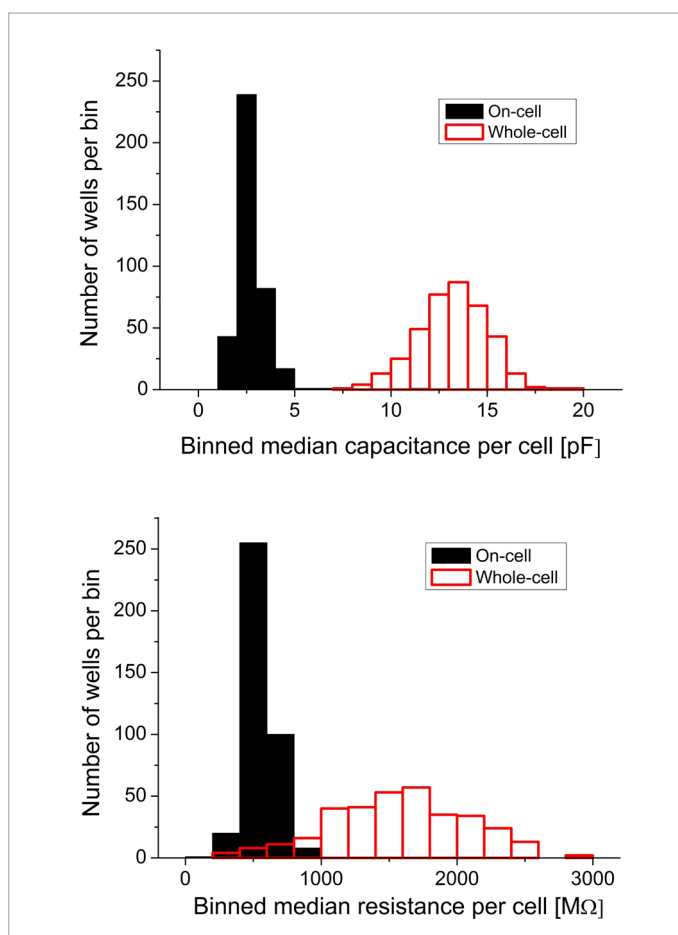
For example, a gain-of-function mutation of Na<sub>v</sub>1.4 can lead to membrane hyperexcitability that causes uncontrolled repetitive muscle fiber discharges and eventually results in myotonia or paralysis (England & De Groot, 2009). Use-dependent inhibitors such as flecainide or other lidocaine analogues can be used in the treatment of some of these conditions as they preferentially inhibit action potentials with high frequencies and thus reduce muscle contractions in the patients (Eijkelkamp et al., 2012).

A high-fidelity patch clamp set up is necessary to discover such a use-dependent drug. Qube is a second generation automated patch clamp system that fulfills this requirement and allows for testing of many thousands of compounds per day in an unattended fashion. Using Qube in a drug development cascade allows to ask the right questions during the primary screen, making a follow-up validation study obsolete.

In the present study, we used the TE671 cell line (ATCC) that endogenously expresses Na<sub>v</sub>1.4 to develop an assay with high success rate and reproducibility, suitable for a high-throughput screening (HTS) campaign.

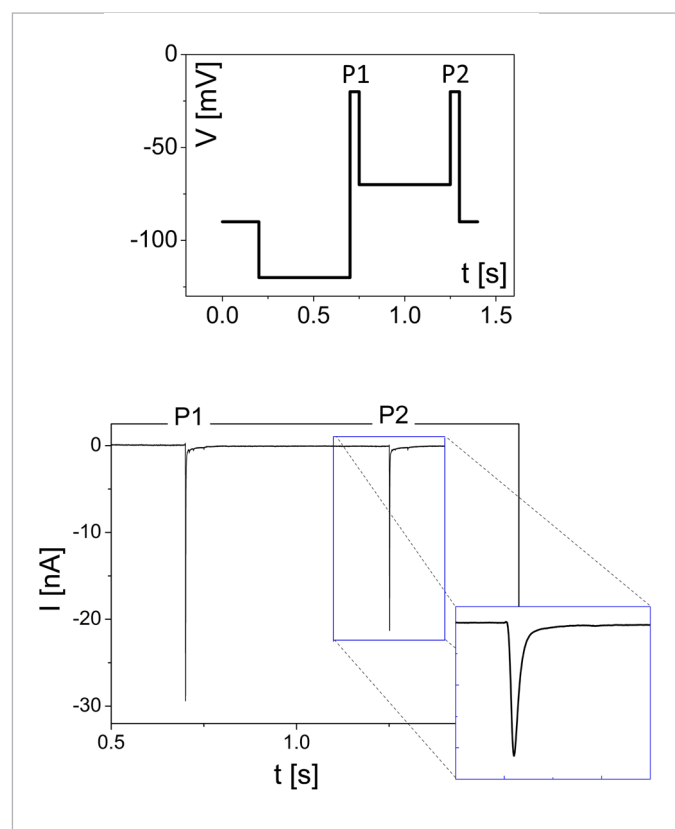
## Results and discussion

A 384-well based HTS assay was developed using the Qube platform that allows for reproducible testing of many thousands of compounds per day. In a first step, quality parameters such as capacitance and seal resistance were determined. Figure 1 shows total capacitance and total resistance before and after application of the whole-cell pressure pulse. As expected, a 4 s long negative pressure pulse to -250 mbar ruptured the membrane patch as indicated by the increase in capacitance. High seal resistances were already measured in the on-cell configuration, additional waiting time and the whole-cell rupture further increased seal resistance resulting in a mean of  $1.5 \pm 0.5 \text{ G}\Omega/\text{cell}$  in the whole-cell configuration.



**Fig. 1:** Median total capacitance (top) and median total resistance (bottom) measured after giga seal formation (black) and following application of a single pressure pulse to -250 mbar for 4 s. The large increase in capacitance after the whole-cell protocol indicates that whole cell access was gained in all cells.

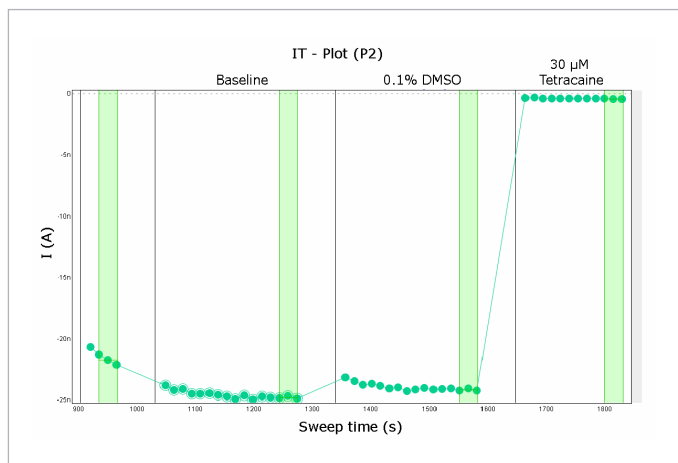
To be able to discriminate between inhibition of different  $\text{Na}_v1.4$  channel states, a partial inactivation protocol was used (Figure 2). A voltage pre-step to -120 mV ensured that the entire channel population was in the closed state prior to a first stimulation (P1) to -20 mV that caused a concerted opening of all channels. A following step to -70 mV kept a portion of the channels in the inactivated state upon a second stimulation to -20 mV (P2). State-dependent inhibitors, such as tetracaine, will preferentially inhibit the inactivated state, thus resulting in a more pronounced inhibition of the peak current measured at the second stimulation following the -70 mV voltage step.



**Fig. 2:** Typical  $\text{Na}_v1.4$  current trace (top) evoked using a partial inactivation voltage protocol (bottom). Cells were clamped at  $V_{\text{hold}} = -90 \text{ mV}$  between voltage protocols. To ensure that all channels were in the closed state prior to stimulation, a pre-pulse to -120 mV for 500 ms was introduced followed by a 50 ms long voltage step to -20 mV (Pulse 1 or P1). Next, cells were clamped at -70 mV for 500 ms before a second voltage stimulation to -20 mV (Pulse 2 or P2). Using such a partial inactivation voltage protocol it was possible to discriminate between closed and inactivated state inhibitors. The voltage protocol was repeated every 15 s.

To study compound effects on Na<sub>v</sub>1.4 a set up was chosen that included a baseline, a test period and a reference period (Figure 3). In more detail, two saline period were applied with 1 and 4 min duration, to establish a stable baseline. During these periods, the voltage protocol described in Figure 2 was continuously applied in 15 s intervals, to monitor changes in peak current. Next, cells were exposed to the test compound or respective negative control for 4 min. Each experiment was finished with application of a supramaximal concentration (on P2) of tetracaine (30 μM) as reference. Average peak currents recorded during the last 3 sweeps of a period were used for further analysis. Relative inhibition was calculated using the following relationship (Equation 1):

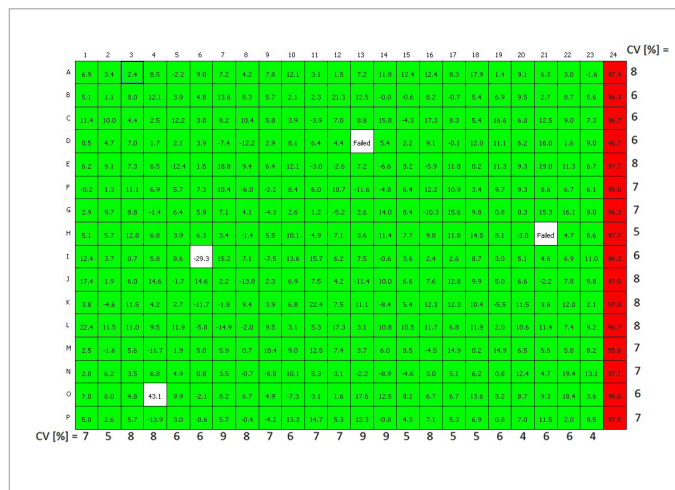
$$\% \text{ Inhibition} = \frac{I(\text{Test}) - I(\text{Baseline})}{I(\text{Reference}) - I(\text{Baseline})} * 100$$



**Fig. 3:** Typical current over time (It) - plot of P2. Following two additions of saline, cells were exposed to a test compound for 4 min (here: 0.1% DMSO). 30 μM tetracaine was used as a reference compound at the end of the experiment. The average values of the three data points shown in the green cursor intervals were used for further analysis. Data were normalized to the value recorded during the baseline period and the reference period.

Studying compound effects on P2 poses often a challenge as for some VGSC assays the voltage for half-inactivation (V1/2) shifts during the experiment. As a result of this, the number of channels that are in the inactivated state when clamped at -70 mV varies throughout the experiment, causing unstable P2 current amplitudes over time. Therefore, we characterized current stability of the Na<sub>v</sub>1.4 assay in a plate uniformity experiment. During this experiment, column 1-23 were exposed to 0.1% DMSO and column 24 was used as positive control with 30 μM tetracaine. Results are shown in Figure 4: the relative current inhibition of P2 is represented for each well of the 384-well QChip. Using this data, coefficient of variation values were calculated for all columns and all rows. All CV values were below the quality criteria of 10%, indicating a high degree of uniformity. The success rate of this experiment, with the filter criteria R<sub>total</sub> > 0.3

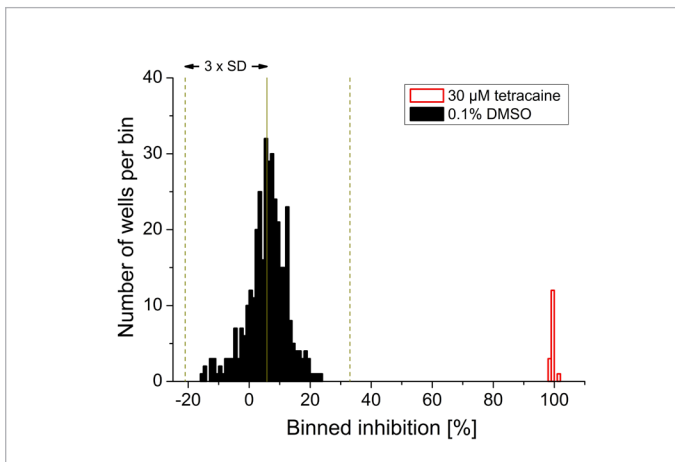
GQ, was 99%. The high quality of the assay is further reflected in the Z' value that was 0.89 and Z = 0.8. Z' was calculated using column 23 and column 24 and input values from column 1-23 as well as column 24 were used to calculate Z.



**Fig. 4:** Plate uniformity experiment. Peak current inhibition of P2 [%], calculated using Equation 1, are shown for each individual well. 0.1% DMSO was applied to column 1-23 and 30 μM tetracaine to column 24. All white wells were failed by the filter criteria, all green wells lie within the mean ± 3 x SD and all red wells show an inhibition ≥ 95%. CV values for the individual columns are shown below the figure and values for the rows (tetracaine excluded) on the right side of the figure. All CV values lie below 10%. The success rate for this experiment was 99% (Filter criteria R<sub>total</sub> > 0.3 GQ). Z' = 0.89 and Z = 0.80.

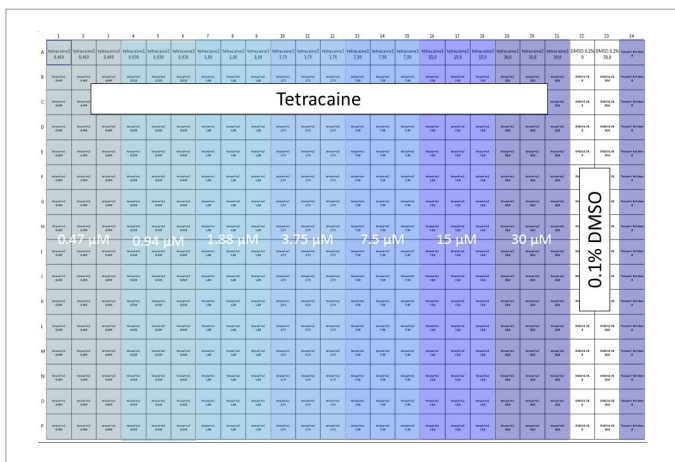
In a large compound screen, a hit is often defined as a compound that inhibits current by more than 3 times the standard deviation (SD) of the negative control. A histogram plot of the relative current inhibition of P2 is shown in Figure 5 with mean and 3 x SD indicated by a bold and a dashed line, respectively. None of the wells receiving DMSO control during the experiment had a value exceeding the 3 x SD (27%) cut-off. Therefore, no false positives were detected in the assay.

In a next step, the assay was characterized pharmacologically using the state-dependent VGSC inhibitor tetracaine. Two different approaches were chosen to record concentration response curves (CRC), a non-cumulative and a cumulative. For the non-cumulative CRC experiment, only one concentration of tetracaine was applied per well and data from several wells were compiled to generate one CRC. For this experiment, the same experimental set up as described in Figure 3 was employed. The cumulative CRC experiment is much more challenging for the assay, as in such an experiment, the whole range of concentrations are applied to each well. This requires a high stability over an extended period of time and through several liquid additions.



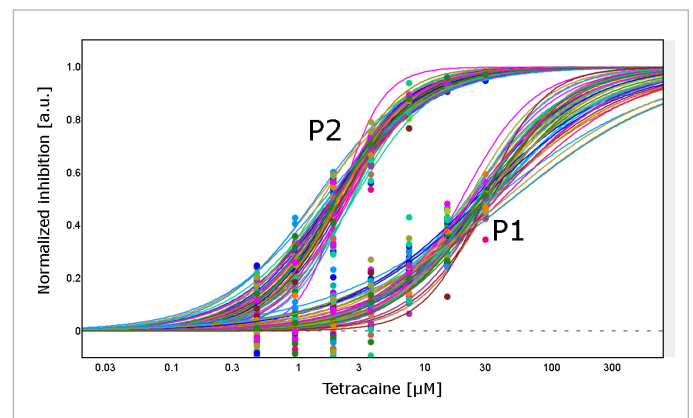
**Fig. 5:** Histogram plot of DMSO control % inhibition data (black) and 30  $\mu\text{M}$  tetracaine (red). The mean % inhibition of DMSO control is shown as bold line and 3 x SD (27%) are indicated with dashed lines. All control data lie within 3 x SD, hence using this cutoff criteria, no false positives were detected in the assay.

Figure 6 shows the compound plate set up used for the non-cumulative concentration response experiment. Each row of a 384-well compound plate contained 7 concentrations of tetracaine in triplicates. Using  $n = 1$  per concentration, it was possible to construct 3 CRCs per row and thus 48 CRCs per experiment. Two negative controls (0.1% DMSO, column 22-23) and a positive control (30  $\mu\text{M}$  tetracaine, column 24) were included to monitor assay stability over time.



**Fig. 6:** Plate set up of a non-cumulative concentration response experiment. 7 concentrations of tetracaine (shown in different shades) were applied to the cell (column 1-21). 0.1% DMSO was added to column 22-23 and 30  $\mu\text{M}$  tetracaine was applied to column 24 as positive control.

Results of the non-cumulative CRC experiment are shown in Figure 7. Both data from P1 and P2 were fitted using a Hill equation. As expected, the highest tetracaine concentration applied (30  $\mu\text{M}$ ) only partially inhibited P1 resulting in a poorly defined CRC. The calculated  $\text{IC}_{50}$  values of P1 ( $\text{IC}_{50} = 30 \pm 6 \mu\text{M}$  (SD;  $n = 48$ )) can therefore only be considered as a rough estimate. In contrast, 30  $\mu\text{M}$  tetracaine completely inhibited  $\text{Na}_v1.4$  – mediated current at P2, confirming its preferential inhibition of the inactivated state. CRCs of P2 are well aligned and exhibit small variation with  $\text{IC}_{50} = 2.0 \pm 0.3 \mu\text{M}$  (SD;  $n = 48$ ; see also Figure 9). The success rate for this experiment, with the filter criteria  $R_{\text{total}} > 0.3 \text{ G}\Omega$ , was 99% and  $Z'$  calculated from column 23 (negative control) and 24 (positive control) was 0.77.



**Fig. 7:** State-dependent inhibition of tetracaine on  $\text{Na}_v1.4$ . Tetracaine exhibits different lower potency on P1 as on P2. 3 individual, non-cumulative, 7 point CRCs were constructed from each row of the set up shown in Figure 6, resulting in 48 CRCs with  $n=1$  per concentration for each P1 and P2. A Hill equation was fitted to the data and the respective  $\text{IC}_{50}$  values for P2 are shown in Figure 9. Note, the maximal applied concentration of tetracaine (30  $\mu\text{M}$ ) only caused a partial inhibition of P1. Therefore, the Hill curve of P1 is not well defined and shows larger variation. The success rate of this experiment, with the filter criteria  $R_{\text{total}} > 0.3 \text{ G}\Omega$ , was 99% and  $Z' = 0.77$ .

A cumulative CRC was recorded using 2 saline periods with 1 and 4 min duration followed by 8 increasing concentrations of tetracaine with each 2 minute exposure time (Figure 8, left). A negative (0.1% DMSO) and positive control (30  $\mu\text{M}$  tetracaine) were added to column 23 and 24, respectively. This set up allowed to record 352 individual CRCs with each 8 concentrations in one experiment (Figure 8, right).  $\text{IC}_{50}$  values calculated from this experiment ( $\text{IC}_{50} = 1.8 \pm 0.4 \mu\text{M}$  (SD;  $n = 348$ ); see also Figure 9) were in line with values obtained for the non-cumulative CRC experiment. Success rate of this experiment was 99% and  $Z' = 0.84$ .

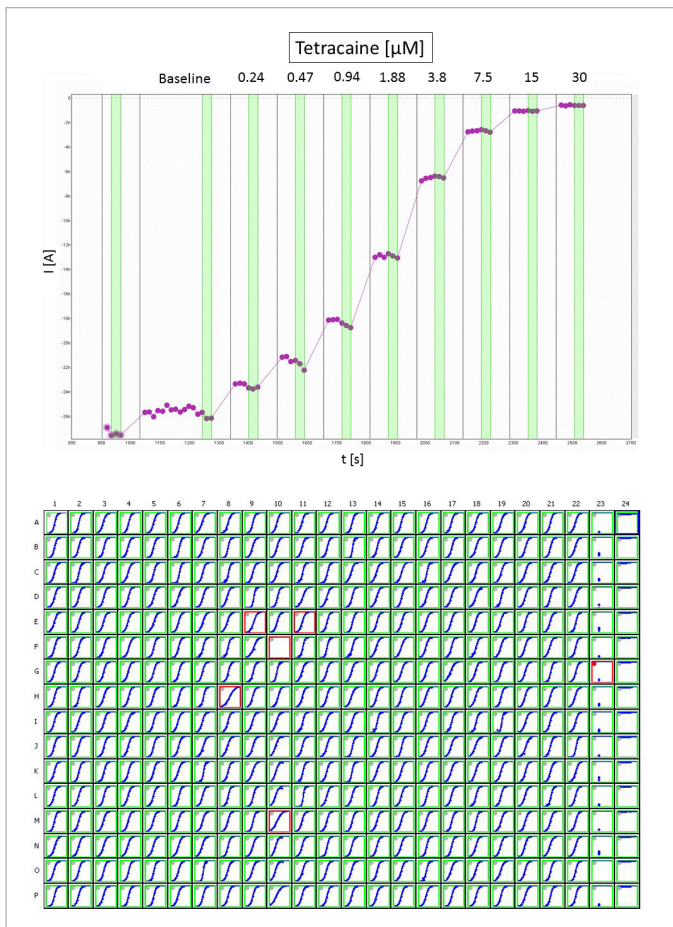


**Fig. 8:** Cumulative, 8 point CRC of tetracaine on P2. Top: P2 peak current over time. Following two saline periods of 1 and 4 min duration, increasing concentrations of tetracaine, as indicated, were applied to each cell. Bottom: Plate view showing individual CRCs of each well. Column 23 and 24 were exposed to a 0.1% DMSO and 30  $\mu\text{M}$  tetracaine control, respectively. The corresponding  $\text{IC}_{50}$  values are presented in Figure 9.

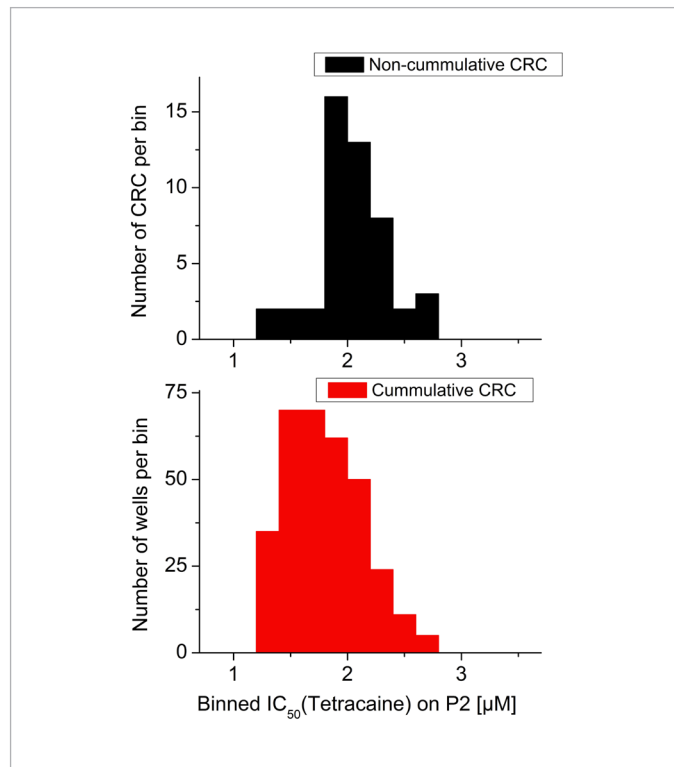


**Fig. 9:** Histogram plot of  $\text{IC}_{50}$  values of tetracaine on P2. Data of the non-cumulative CRC are shown in the upper panel (data from Figure 7), values calculated from cumulative CRCs are shown in the lower panel (data from Figure 8).  $\text{IC}_{50}$  values of both approaches were in good agreement with each other with  $\text{IC}_{50} = 2.0 \pm 0.3 \mu\text{M}$  (SD;  $n = 48$ ) for the non-cumulative and  $\text{IC}_{50} = 1.8 \pm 0.4 \mu\text{M}$  (SD;  $n = 348$ ) for the cumulative concentration response experiment.

## Methods

### Cells

- TE671 cells endogenously expressing Nav1.4 were cultured at 37°C and 5% CO<sub>2</sub> in Dulbecco Modified Eagle Medium (DMEM) supplemented with 10% fetal bovine serum (FBS), 100 U/ml Penicillin and Streptomycin, and 2 mM sodium-pyruvate. Cells were purchased at ATCC.

On the day of the experiment, cells were harvested using Detachine and kept in serum-free media until further use. Qube's automated cell preparation unit was used to resuspend cells in saline just before the start of the experiment.

### Electrophysiology

- Whole cell access was gained using a single pressure pulse to -250 mbar for 4 s. Cells were afterwards clamped at V<sub>hold</sub> = -90 mV and -10 mbar.
- All experiments were done using multihole QChips (10 holes / well).
- Data was analyzed using Sophion's Analyzer and Origin 7.5 (OriginLab) software. Data are represented as mean ± SD.

### References:

- Eijkelkamp, N., Linley, J. E., Baker, M. D., Minett, M. S., Cregg, R., Werdehausen, R., ... Wood, J. N. (2012). Neurological perspectives on voltage-gated sodium channels. *Brain*, 135(9), 2585–2612. <http://doi.org/10.1093/brain/aws225>
- England, S., & De Groot, M. J. (2009). Subtype-selective targeting of voltage-gated sodium channels. *British Journal of Pharmacology*, 158(6), 1413–1425. <http://doi.org/10.1111/j.1476-5381.2009.00437.x>
- Jurkat-Rott, K., Holzherr, B., Fauler, M., & Lehmann-Horn, F. (2010). Sodium channelopathies of skeletal muscle result from gain or loss of function. *Pflügers Archiv European Journal of Physiology*, 460(2), 239–248. <http://doi.org/10.1007/s00424-010-0814-4>
- Yu, F. H., & Catterall, W. a. (2003). Overview of the voltage-gated sodium channel family. *Genome Biology*, 4(3), 207. <http://doi.org/10.1186/gb-2003-4-3-207>

### Author:

Daniel R Sauter, Application scientist

Sophion Bioscience A/S, Baltorpevej 154, 2750 Ballerup, Denmark  
Phone: +45 4460 8800 Fax: +45 4460 8899, E-mail: [info@sophion.com](mailto:info@sophion.com)

[sophion.com](http://sophion.com)